Software Defined Radio Implementation of a Non-Orthogonal Multiple Access System Towards 5G

Xingguang Wei*, Haitao Liu*, Zhiming Geng*, Kan Zheng*, *Senior Member, IEEE*, Rongtao Xu†, Yang Liu‡, Peng Chen‡

*Intelligent Computing and Communication (IC^2) Lab
Key Lab of Universal Wireless Communications, Ministry of Education
Beijing University of Posts & Telecommunications
Beijing, China, 100088
†State Key Laboratory of Rail Control and Safety
Beijing Jiaotong University
Beijing, China, 100044
‡Technology Innovation Center of China Telecom Corporation Limited
Beijing, China, 102209

Contact email: zkan@bupt.edu.cn

***Abstract*—Non-orthogonal multiple access (NOMA) is envisioned to be one of essential technologies for the fifth generation (5G) mobile network. In this article, we implement a practical downlink NOMA system by means of software defined radio (SDR) based on OpenAirInterface (OAI). For comparison purpose, our SDR-based NOMA system follows the basic specifications of long term evolution (LTE). In this system, a codeword-level successive interference cancellation (SIC) receiver is implemented. To improve the efficiency of baseband signal processing in SIC receiver, a multi-thread processing method is also introduced. Due to the limitation of original downlink control information (DCI) formats in current LTE systems, a new DCI format is dedicatedly designed for signal reconstitution in our developed NOMA system. Furthermore, some parts of upper layer protocols in LTE system are modified to support the application services over the developed NOMA system. Based on our NOMA system, a series of over-the-air experiments are carried out, and the experiment results demonstrate that the NOMA scheme has a significant throughput gain compared with orthogonal multiple access (OMA) scheme.**

***Index Terms*—5G, LTE, NOMA, OAI, SDR.**

I. Introduction

MULTIPLE access scheme allows multiple users to share the limited wireless resource and to communicate with each other at the same time. To further improve the capacity and spectrum efficiency of the fifth generation (5G) mobile network [1], the non-orthogonal multiple access (NOMA) has become the hotspot due to its higher spectrum efficiency and larger capacity compared with the orthogonal multiple access (OMA) [2]. For example, a new study item termed as the multiuser superposition transmission (MUST), i.e., some kind of downlink NOMA, has been established in Release 13 by the 3rd generation partnership project (3GPP) standardization body [3]. Different from the traditional multiple access techniques adopted in the current mobile networks, which rely on the time/frequency/code domain, NOMA explores a new non-orthogonal domain to distinguish signals from several different users, i.e., power domain. In the NOMA scheme, the signals of multiple users are superposed in power domain at the transmitter side, and the signal separation of different users is realized via successive interference cancellation (SIC) at the receiver side [4].

To further evaluate the performance of practical NOMA system, the software defined radio (SDR) provides a flexible and inexpensive solution for rapidly prototyping a practical NOMA system and characterizing its performance. The concept of SDR is to implement the components of communications system by means of software [5]. In particular, the general purpose processor (GPP) based SDR system can be efficiently implemented and updated with the help of high level programming languages [6], e.g., C/C++, Java and Python. In the last decades, a plenty of SDR projects are being rapidly developed in an open-source approach, e.g., OpenBTS [7], srsLTE [8] and so on. Among them, OpenAirInterface (OAI) [9] might be the most attractive open source platform, in which the evolved node B (eNB), user equipment (UE) and evolved packet core (EPC) are being fully developed according to the 3GPP specification [10].

To the best of the authors' knowledge, most of the existing study related to NOMA focuses on the theoretical analysis and simulation[11] [12], the over-the-air performance of NOMA system has not been well evaluated so far. Furthermore, almost all the existing NOMA systems are only focused on the design of physical (PHY) and medium access control (MAC) layers [13] [14], there still remains a lot of issues and challenges on the upper layer protocols design for NOMA system. In this article, a practical downlink NOMA system is implemented by means of SDR based on the physical layer of OAI. For fair comparison with OMA system, our developed NOMA system follows the basic specifications of long term evolution (LTE). In our NOMA system, a codeword-level SIC receiver is implemented for robust multiple access [13], in which the multi-thread processing method is designed to improve its efficiency of baseband signal processing. Due to the adoption of SIC receiver, the original downlink control information

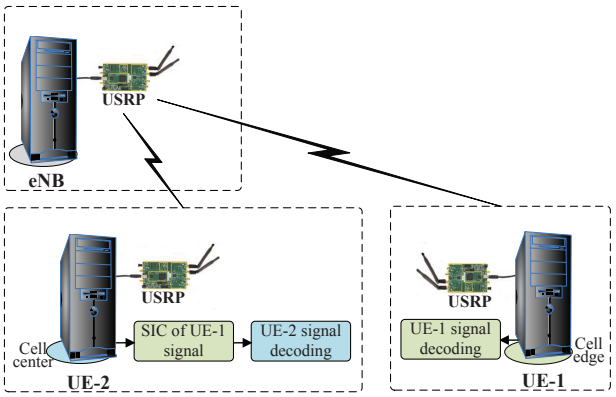

Fig. 1. Deployment scenario of SDR-based NOMA system.

(DCI) formats in LTE systems cannot be directly applied in NOMA system. Thus, a new DCI format is specially designed for signal reconstitution in our developed NOMA system. Moreover, some parts of upper layer protocols in LTE system are modified to support the application services over our NOMA system. Finally, some over-the-air experiments are carried out to validate the feasibility of applying NOMA in practical wireless communications systems towards 5G.

The remainder of this article is organized as follows. Section II describes the design and implementation of our NOMA transceiver which elaborates on three parts, i.e., NOMA transceiver, multi-thread processing method and new DCI format for NOMA system. Then, Section III introduces the modification on upper layer protocols in NOMA system. Over-the-air experimental results carried out with our NOMA system are presented in Section IV. Finally, concluding remarks are drawn in Section V.

II. Design and Implementation of a NOMA Transceiver

The new transceiver needs to be designed to support the superposition, reconstitution and cancellation in NOMA system, which is implemented by introducing new communications modules to the OMA eNB and UE in OAI platform. Especially, we focus on the implementation of the transceiver on physical downlink shared channel (PDSCH). For a better understanding of our proposed NOMA system, the NOMA transceiver is introduced by theoretical analysis and practical implementation in the first subsection. Then, the multi-thread processing method on UE receiver is proposed to improve its efficiency of baseband signal processing. Finally, the design of a new DCI format for NOMA system is presented.

A. NOMA transceiver

Fig. 1 illustrates the deployment scenario of our proposed NOMA system with single-input single-output (SISO) transmission mode. The eNB serves only two UEs, i.e., the cell-edge UE and the cell-center UE. For ease of exposition, the cell-edge UE and cell-center UE are represented as UE-1 and UE-2 in this article, respectively. Either the eNB or UE consists of a GPP and a universal software radio peripheral (USRP). The GPP executes the programs that process the digital baseband signals, e.g., scrambling, turbo encoding and soft demodulation. The baseband signal processing programs can be efficiently developed by using high-level programing languages and open source libraries [15] [16]. For another, USRP is one of the most widespread peripheral equipment in SDR systems. The USRP is mainly for frequency conversion and analog-digital conversion [5], i.e., the digital baseband signal is sent to USRP to be converted to analog one and then up converted to the target RF frequency on the transmit path, and the receive path operates reversely as the transmit path.

As our NOMA system follows the basic specifications of LTE, the modules of encoding/decoding, scrambling/unscrambling, modulation/demodulation and orthogonal frequency division multiplexing (OFDM)/OFDM demodulation in our NOMA transceiver are the same as that in LTE systems [17]. Take the encoding module which is shown in Fig. 2 for example, the encoding module contains code block segmentation, Turbo encoding and rate matching. For another example, the modulation module employs quadrature phase-shift keying (QPSK), 16 quadrature amplitude modulation (16QAM) or 64QAM according to the corresponding DCI.

1) Transmitter: The signals transmitted for UE-1 and UE-2 are superposed at the eNB side according to the power allocation coefficients, which is given by

$$s = \sqrt{1-\alpha}s_1 + \sqrt{\alpha}s_2, \tag{1}$$

where s_1 and s_2 are the normalized signals for UE-1 and UE-2, respectively. $(1-\alpha)$ and α denote the power allocation coefficients. The power allocation coefficient is determined by user channel gain, i.e., the user with poorer channel condition gets more transmission power [18]. As mentioned above, UE-1 is located at the cell edge and UE-2 is located at the cell center. Thus, we assume that UE-2 has a higher channel gain than UE-1. More specifically, UE-1 gets more transmission power than UE-2 in our NOMA system, i.e.,$\alpha < 0.5$.

On the basis of the theoretical derivation above, the NOMA transmitter is implemented by redesigning the communications modules based on OAI eNB. As illustrated in Fig. 2(a), the physical service data units (PSDUs) of the two paired UEs are encoded, scrambled and modulated into complex-valued modulation symbols separately. Then, the modulation symbols of two UEs are allocated with different power according to the power allocation coefficients. As shown in the process of superposition, the symbols of two UEs are superposed in power domain. After superposition, the superposed symbols of two UEs are mapped to the same RBs according to the DCI transmitted in the physical downlink control channel (PDCCH). Differently, the PDCCH signals are not superposed in power domain at the transmitter. Thus, the DCI symbols are generated by each UE separately and mapped to different RBs. Finally, all these symbols are modulated to OFDM symbols and then transmitted by a USRP.

2) Receiver: At the receiver, the received superposed signal can be separated via SIC. The SIC receiver detects the signal of one UE by either zero force (ZF) or minimum mean square error (MMSE) principle, and subtracts the detected signal from the received superposed signal to cancel its interference for the

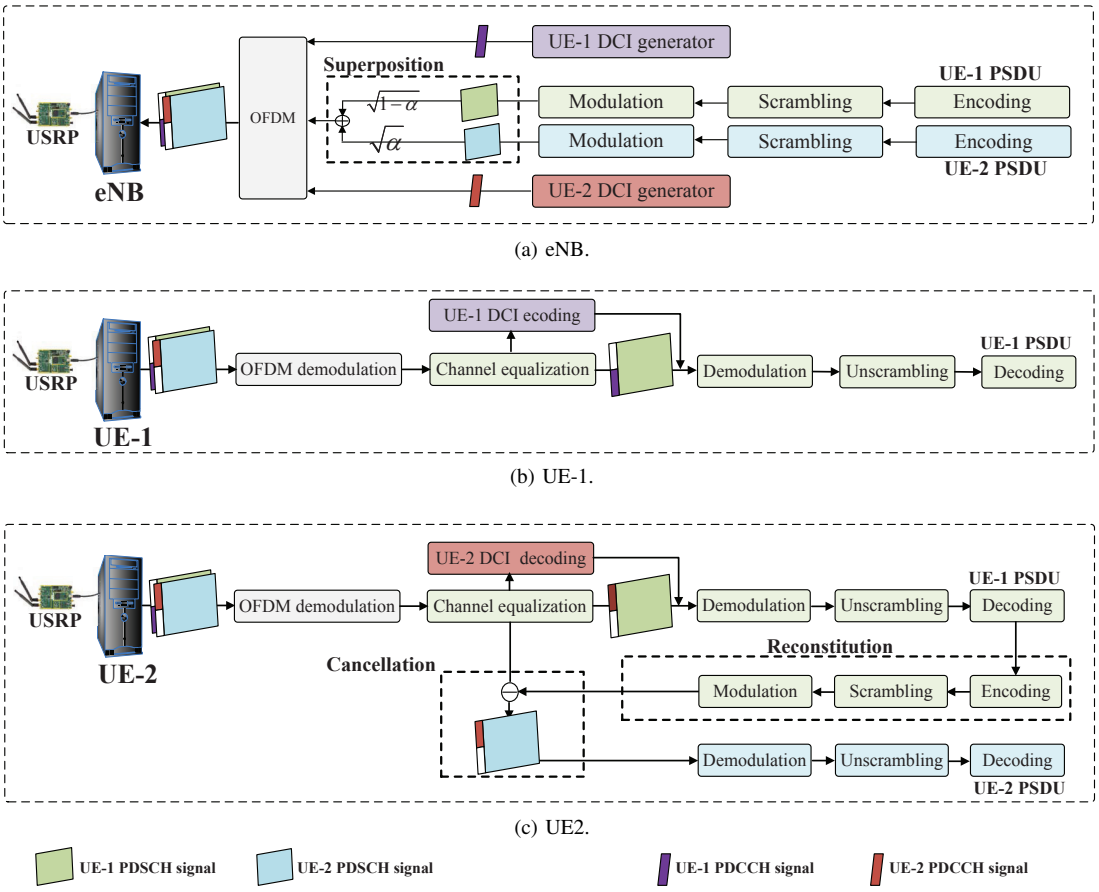

Fig. 2. Implementation of NOMA transceiver.

other undetected signals, then detects the signal of the next UE until all the signals have been detected [13]. The ZF principle is employed in our NOMA system due to its low computation complexity.

a) UE-1: After going through the wireless channels, the signal received by UE-1 is represented as

$$y_1 = h_1(\sqrt{1-\alpha}s_1 + \sqrt{\alpha}s_2) + n_1, \tag{2}$$

where h_1 is the channel matrix, and n_1 is the noise of UE-1. The UE-1's signal has been allocated with more transmission power, which ensures UE-1 to detect its signal directly by regarding the UE-2's signal as noise. The detailed detection steps are as follows.

- **STEP 1: Detection by ZF principle**

$$\hat{s} = h_{ZF}y_1 = h_{ZF}(h_1\sqrt{1-\alpha}s_1 + (h_1\sqrt{\alpha}s_2 + n_1)), \tag{3}$$

where h_{ZF} is the estimated channel matrix by ZF principle and $h_{ZF} = {s_1}^{-1}y_1$.

- **STEP 2: Normalization**

$$\hat{s}_1 = \frac{\hat{s}}{\sqrt{1-\alpha}}, \tag{4}$$

where $\hat{s}_1$ is the detected signal of UE-1. $\hat{s}$ and $\hat{s}_1$ are of the same performance in terms of soft demodulation because the linear change of signal does not influence its performance [19].

As shown in Fig. 2(b), the UE-1 receiver in the proposed NOMA system is the same as the UE receiver in LTE systems, i.e., it is the same as the OAI UE receiver. Firstly, the received superposed signal is transfered from USRP to GPP via the interface of universal serial bus (USB) 3.0. Then, the received superposed signal is demodulated into symbols by OFDM demodulation. After that, UE-1 detects its signal by ZF principle in channel equalization by regarding the UE-2's signal as noise. As we can see, the STEP 2 is not implemented in the UE reciever due to the adoption of soft demodulation. After channel equalization, the DCI information is detected and decoded for further decoding the UE-1 PSDU. Finally, the UE-1 PSDU is extracted by demodulation, unscrambling and decoding according to information carried by DCI.

b) UE-2: On the other side, the signal received by UE-2 is expressed by

$$y_2 = h_2(\sqrt{1-\alpha}s_1 + \sqrt{\alpha}s_2) + n_2, \tag{5}$$

where h_2 denotes the channel matrix, and n_2 denotes the noise of UE-2. Different from the UE-1 receiver, a codeword-level SIC receiver is implemented at the UE-2 receiver due to its better performance than symbol-level SIC [13]. The UE-2 needs to firstly detect UE-1's signal and then subtracts this signal from the received superposed signal before decoding its own message. The detailed detection steps are as follows.

- **STEP 1: Detection by ZF principle**

$$\hat{s} = h_{ZF}y_2 = h_{ZF}(h_2\sqrt{1-\alpha}s_1 + (h_2\sqrt{\alpha}s_2 + n_2)), \tag{6}$$

where h_{ZF} is the estimated channel matrix by ZF principle and $h_{ZF} = {s_1}^{-1} y_2$.

- **STEP 2: Normalization**

$$\hat{s}_1 = \frac{\hat{s}}{\sqrt{1-\alpha}}, \tag{7}$$

where $\hat{s}_1$ is the detected signal of UE-1. As mentioned above, this is an optional step in our NOMA system because $\hat{s}$ and $\hat{s}_1$ are of the same performance in soft demodulation.

- **STEP 3: Decoding and Reconstitution**

Decoding the bit sequence of UE-1 by turbo decoding as turbo decoding can enhance the reliability of every bit [13]. With appropriate power coefficients, the UE-1 PSDU can be decoded successfully. Then, in the process of reconstitution, the UE-1 PSDU is encoded and modulated as $\breve{s}_1$ to reconstitute the modulated symbols of UE-1.

- **STEP 4: Cancellation**

Cancelling the $\breve{s}_1$ from $\hat{s}$ as

$$\hat{s}_2 = \frac{\hat{s} - \sqrt{1-\alpha}\breve{s}_1}{\sqrt{\alpha}}, \tag{8}$$

where $\hat{s}_2$ is the detected signal for UE-2.

As shown in Fig. 2(c), the theoretical analysis is mapped to the implementation of UE-2 receiver. The UE-2 receiver firstly decodes the received superposed signal as same as the UE-1 receiver. As the process of reconstitution shown, the decoded UE-1 PSDU is then encoded and modulated again to reconstitute the modulated symbols through the same processes as the signal transmission of UE-1 at the eNB side, i.e., DLSCH encoding, scrambling, and modulation. After reconstitution, the UE-1's signal is canceled from the received signal after channel equalization in the process of cancellation. Finally, the UE-2 receiver can demodulate and decode the signal intended for itself by soft demodulation, unscrambling and turbo decoding.

B. Multi-thread Processing Method

The original OAI UE receiver is single-thread processing. As a result, the UE must receive and decode the signal of each subframe serially within one transmission time interval (TTI) accurately, i.e., 1 *ms* [20]. If the time that GPP consumes to process the signal of one subframe exceeds 1 *ms*, the time slot of next subframe will be occupied ended with losing synchronization with eNB. In the downlink NOMA system, decoupling the superposed signal of multiple users is realized by SIC receiver at the UE side. There are several key baseband signal processing modules in a SIC receiver including signal decoding, reconstitution and cancellation, and all these modules are of high computation complexity. Moreover, the computation complexity grows higher with the increase of system bandwidth and the number of paired UEs in NOMA system [2].

In order to efficiently carry out the baseband signal processing in real time, the multi-thread processing method is introduced to our proposed NOMA UE receiver [21]. As shown in Fig. 3, ten threads are established for UE receiver, where each thread deals with the data within one subframe. The thread

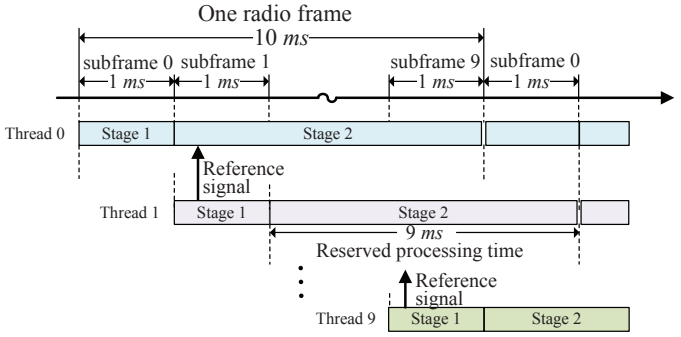

Fig. 3. Multi-thread processing method for UE receiver.

number is corresponding to the subframe number. Considering that the lease square (LS) is used as the channel estimation method in OAI, which utilizes a part of reference signal from next subframe to improve the channel estimation accuracy of the current subframe, each thread is divided into 2 stages, i.e., Stage 1 and Stage 2. The OFDM demodulation is realized in Stage 1 and the rest processing procedures are realized in Stage 2. When the Stage 1 has completed, the thread steps into Stage 2 waiting for the reference signal from next subframe to start channel estimation, and continues completing the rest processing procedures as soon as the reference signal from next subframe arrives. For example, thread 0 has finished the OFDM demodulation and stepped into Stage 2 waiting for the reference signal form thread 1. As the reference signal from thread 1 arrives, the thread 0 continues finishing the rest processing procedures, e.g., channel equalization, DCI decoding, reconstitution and cancellation.

The multi-thread processing method allows more time for UE to receive and decode the data of each subframe, which improves its potential for being applied in high-throughput scenarios. Although the downlink hybird automation repeat request (HARQ) feedback has to be transmited within 4 TTI (4 *ms*) in the LTE frequency-division duplexing (FDD) systems [22], the reserved processing time of Stage 2 for each subframe can be extended to 9 *ms* irrespective of the HARQ process.

C. New DCI Format

As has been explained in subsection A, the UE-1 receiver is the same as the UE receiver in LTE systems. In other words, the DCI formats in LTE systems can be directly used for UE-1 in NOMA system. Unlike the UE-1 receiver, the codeword-level SIC is adopted in UE-2 receiver. The UE-2 receiver has to firstly decode and reconstitute the UE-1's signal before it can demodulate and decode the signal intended for itself. Consequently, a new DCI format that contains some additional information of UE-1 needs to be designed for UE-2.

In our NOMA system, UE-1 employs the DCI format 1A. For another, a new DCI format based on DCI format 1A is designed and implemented for UE-2, which contains some additional fields for UE-2 receiver to decode and reconstitute the UE-1's signal. The new DCI format is named as DCI format 1E, and the detailed fields of DCI format 1E (5MHz) are shown in Table I. *Power allocation ratio* indicates the

TABLE I
DCI FORMAT 1A (5MHZ) AND DCI FORMAT 1E (5MHZ)

Field name	DCI format 1A length (Bits)	DCI format 1E length (Bits)
Format 0 / Format1A flag	1	1
Localized / Distributed VRB assignment flag	1	1
Resource block allocation	9	9
MCS	5	5
HARQ process	3	3
New data indicator	1	1
Redundacy version	2	2
TPC for PUCCH	2	2
Power allocation ratio	**–**	**3**
MCS for paired UE	**–**	**5**
RV for paired UE	**–**	**2**

power allocation coefficients, which can provide 8 power allocation schemes at most by 3 bits. For example, 111 represents the power allocation coefficients (1/4, 3/4) in our proposed NOMA system, i.e., the UE-1 is allocated with three quarters of the total power, and the rest power is allocated to the UE-2. *MCS for paired UE* refers to the modulation and coding scheme (MCS) of UE-1, which is an essential parameter for UE-2 receiver to demodulate UE-1's signal. *RV for paired UE* represents the redundancy version (RV) of UE-1 that used for rate matching in turbo decoder/encoder. Furthermore, the C-RNTI of UE-1 is indispensable for UE-2 receiver to check the cyclic redundancy check (CRC) answer of UE-1's signal. The C-RNTI is of 16 bits length in LTE systems, which is too long to consist in DCI for the reason that the complexity of DCI detection in UE receiver is proportion to the length of DCI [23]. Currently, the C-RNTIs of UE-1 and UE-2 are manually set in our NOMA system to reduce the DCI detection complexity.

III. UPPER LAYER PROTOCOLS FOR NOMA

Without the deployment of EPC, some parts of upper layer protocols of the current LTE systems have to be modified to provide the application services over our NOMA system [24]. As shown in Fig. 4, the protocol stack of NOMA system contains seven layers, which from top to bottom are as follows, i.e., application layer, transport layer, network layer, packet data convergence protocol (PDCP), radio link control (RLC), MAC and PHY. Benefit from the transparent transmission of our proposed protocol stack, our NOMA system can provide all kinds of application services, such as voice, video, data and so on.

The application layer, transport layer and network layer are the same as that in transmission control protocol/Internet protocol (TCP/IP) protocol stack. The application layer provides a interface for application services, which contains the interface methods used in process-to-process communications across an IP computer network. The transport layer provides host-to-host communication services for applications, such as connection-oriented data stream support, reliability, flow control and so on. The network layer is responsible for packet forwarding including routing through intermediate routers. Each of the three layers adds a packet header to the input service data

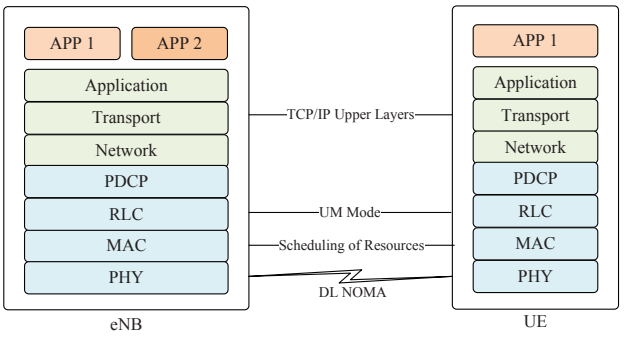

Fig. 4. Protocol stack of NOMA system.

unit (SDU) to generate the output protocol data unit (PDU) at the transmitter side, and then removes the packet header from the PDU to generate the SDU at the receiver side.

As for the PDCP and RLC, they are the same as that in LTE protocols. However, the MAC and PHY have been elaborately redesigned for the proposed NOMA system. The PDCP is mainly used for header compression of PDU generated by the network layer. Unfortunately, the PDCP in our NOMA system is still unfinished, which will decrease the traffic transmission efficiency to some extent. The RLC layer segments and concatenates the data packet from the PDCP according to the transport block size (TBS), and recovers the data packet at the receiver side. The unacknowledged mode (UM) RLC has been accomplished in our NOMA system. The MAC is the wireless resource scheduling center of NOMA system, which pairs UEs and computes the best power allocation coefficient for each UE according to their reported channel quality indicator (CQI). For simplicity, the two UEs are paired manually in our NOMA system. The PHY is responsible for transmitting and receiving the superposed signal between eNB and UEs.

IV. EXPERIMENTAL RESULTS AND ANALYSIS

A. System Configuration

As shown in Fig. 5, the three general purpose computers are of the similar configuration and the computer of eNB is taken as an example to illustrate the system configuration. The CPU model of general purpose computer is Intel(R) Core(TM) i7-4770, which has four physical cores supporting hyper-threading. Moreover, the maximum clock frequency of CPU is 3.4 GHz, which is powerful enough to satisfy the computational requirement of our NOMA system. Even more important, the cores support the streaming SIMD extensions (SSE) and advanced vector extensions (AVX) instruction sets for parallel computing, which can improve the program efficiency at run time for the reason that some algorithms in OAI are written by SSE and AVX. As for the operating system (OS), the 64-bit Ubuntu 14.04 is installed in these computers.

The USRP B200 is selected as the peripheral equipment due to its flexibility in SDR LTE platform, whose sampling rate is a multiplier of all the sampling rates defined in 3GPP LTE specifications, i.e., 61.44MHz. Moreover, the USPR B200 supports continuous frequency coverage from 70 MHz to 6 GHz, which can operate on all LTE frequency bands. The RX

gain of USRP is set to adjust the amplification of the RX antenna, which has a great effect on the quality of received signal. Low-level RX gain leads to weakness of received signal, resulting in detection failure. Though, high-level gain brings about highly increased system noise.

Some of the system configuration parameters are shown in Table II. The power allocation coefficients are fixed at (1/4, 3/4) in the proposed NOMA system. There are only 8 subframes used to transmit the user traffic data in our NOMA system, since the subframe 0 and subframe 5 are dedicated to transmit the system information/signal, such as system broadcast information, primary synchronization signal (PSS), secondary synchronization signal (SSS) and so on.

TABLE II
EXPERIMENTAL SCENARIOS PARAMETERS

Parameter		Value
Duplex mode		FDD
Transmission mode		TM1 (SISO)
DL Carrier frequency		2.68 GHz (band7)
System bandwidth		5 MHz
Subframes for user traffic in one frame		8
Power allocation coefficients		(1/4,3/4)
eNB TX gain		90 dB
Distance from eNB	UE-1	1 m
	UE-2	2 m
Best MCS	UE-1	9
	UE-2	25
RX gain	UE-1	75 dB
	UE-2	95 dB

B. Experimental Scenarios

In order to make performance comparisons between OMA and NOMA system, the experimental scenarios are deployed to measure the peak throughput of OMA system. The original OAI is a typical SDR platform of LTE Release 8 specifications, which is used as the OMA system in our experiment. For fair comparisons, the throughput of NOMA system is measured in the same experimental scenarios. Then, the performance comparisons between OMA and NOMA system are carried out.

In our experimental scenarios, the UE-2 is in the cell center with a high channel gain, which can use 64QAM (MCS 17-28); the UE-1 is in the cell edge with a low channel gain, which can only utilize the QPSK (MCS 0-9). For the limitation of experimental space, the UE-2 is placed 1 meter away from the eNB and the UE-1 is placed 2 meters away from the eNB. In OMA system, we assume that the best MCS of UE-1 is 9 and the best MCS of UE-2 is 25 in our experimental scenarios. The best MCS is defined as the MCS that gives the maximum average downlink (DL) throughput for each UE. However, the RX gain of USRP has a great influence on the received signal quality and then further influences the best MCS of UE. So far, the adaptive modulation and coding (AMC) has not been realized in our NOMA system [25], and the best MCS has to be measured manually .

To deploy the experimental scenarios that the best MCS of UE-1 is 9 and the best MCS of UE-2 is 25, the origin OAI is used to adjust the RX gain of each UE. Firstly, the TX gain of eNB is fixed at 90 dB and the DL MCS is fixed at 9, then the UE-1 is accessed to eNB alone by OMA with all the wireless resource allocated to it, i.e., 8 subframes and 25 RBs. As the RX gain of UE-1 gradually increased, the average DL throughput of UE-1 reaches its maximum when the RX gain is set to 75 dB, i.e., 3.2 Mbps. The average DL throughput is measured within 10000 frames over the air, and the throughput in this article is all referred to the average DL throughput. Similarly for UE-2, when the RX gain is set to 95 dB, the UE-2 throughput becomes the highest, i.e., 11.2 Mbps. The experimental scenarios are summarized in Table II.

C. Performance Comparisons

1) OMA: As mentioned above, the peak throughput of OMA system can be measured in our experimental scenarios with two UEs accessing the eNB via OMA at the same time. However, the throughput of OMA system is affected by the wireless resource allocation scheme. For convenience, the subframe is utilized as the minimum scheduling unit in NOMA system. In the practical cellular system, user with poorer channel condition gets less wireless resource for maximizing the system throughput. Accordingly, we assume that 4/8 at most of the total subframes are allocated for UE-1. The UE-1 throughput, UE-2 throughput and system throughput have been measured under the assumption that only 0/8, 1/8, 2/8, 3/8 and 4/8 of the total subframes are allocated for UE-1 and the rest are allocated for UE-2, where the system throughput refers to the total throughput of UE-1 and UE-2.

As shown in the Fig. 6, the UE-1 throughput increases slowly while the UE-2 throughput decreases quickly as the wireless resource allocated for UE-1 increases. As a result, system throughput decreases as the wireless resource allocation ratio for UE-1 increases. For maximizing system throughput, the UE-1 is hardly scheduled. The system throughput reaches its maximum with all the wireless resource allocated for the UE-2, i.e., 11.2 Mbps.

2) NOMA: In NOMA system, the power allocated for each UE decreases compared with the OMA system. In return, two UEs can share all the time-frequency resource at the same time. To measure the peak system throughput of NOMA system, all the 120 pair schemes of UE-1 and UE-2 have to be tested, i.e., the pair schemes of UE-1 with MCS set to 0-9 and UE-2 with MCS set to 17-28. In our experimental scenarios, two UEs access the eNB via NOMA at the same time. The UE-1 throughput, UE-2 throughput and system throughput have been measured. For a better illustration of the results, only the throughput curves that the MCS of UE-1 is set to 5-9 are displayed in Fig. 7.

As shown in Fig. 7(a), the UE-1 throughput gradually increases as the MCS of UE-1 increases, and becomes the highest as the MCS of UE-1 is set to 7, i.e., 2.5 Mbps. When the MCS of UE-1 is further increased, the UE-1 throughput decreases and changes acutely. In other words, the best MCS of UE-1 is 7 in our NOMA system. The best MCS of UE-1 decreases a little for the fact that only 3/4 of the power is allocated for the UE-1.

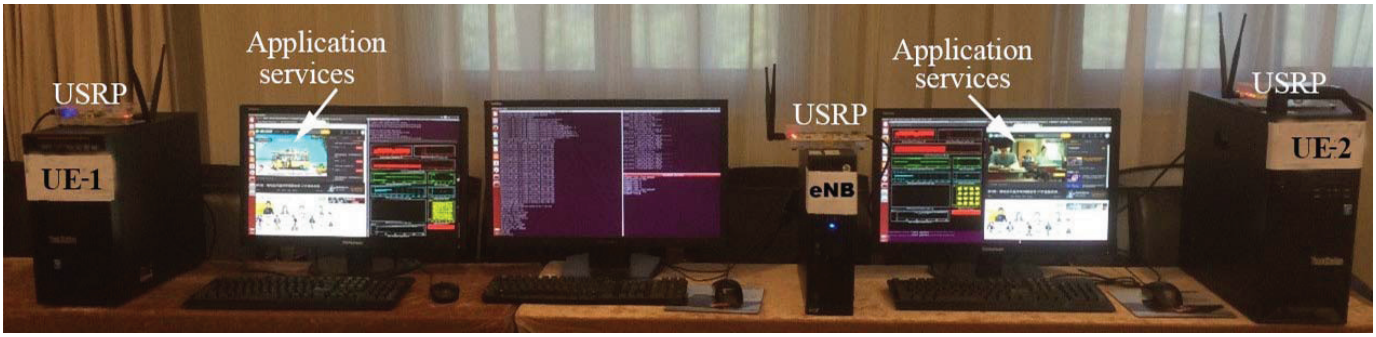

Fig. 5. Experiment environment of our NOMA system.

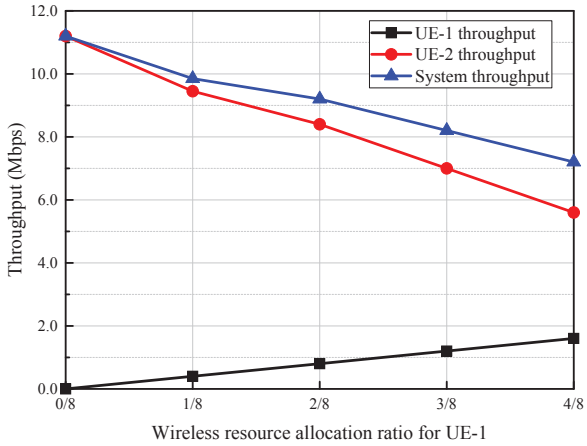

Fig. 6. Throughput of OMA system.

As shown in Fig. 7(b), the UE-2 throughput increases at first as the MCS of UE-2 increases, and reaches the highest throughput as the MCS of UE-2 is set to 25, i.e., 11.1 Mbps, which is slightly smaller than that in OMA system. When the MCS of UE-2 is further increased, the UE-2 throughput decreases sharply. The best MCS of UE-2 in NOMA system is the same as that in OMA system, i.e., 25. Although the power allocated for UE-2 has been decreased by 3/4, it has limited influence on UE-2 throughput due to its good channel condition and appropriate power allocation coefficient.

As shown in Fig. 7(c), the trend of system throughput is similar to UE-2 throughput. The peak system throughput is reached as the MCS of UE-1 is 7 and MCS of UE-2 is 25, where the UE-1 throughput is 2.172 Mbps and the system throughput is 13.279 Mbps.

The peak system throughput comparison and the UE-1 throughput comparison between OMA and NOMA system are summarized in Table III. The throughput gain changes as the wireless resource allocation scheme in OMA system changes. The system throughput gain grows higher as the wireless resource allocation ratio for UE-1 increases. With all the resource allocated for UE-2, the system throughput gain reaches its minimum, i.e., 18.6%; and the system throughput gain reaches its maximum as 4/8 of the resource is allocated for UE-1, i.e., 84.4%. On the contrary, the UE-1 throughput gain grows lower as the wireless resource allocation ratio for UE-1 increases. When 4/8 of the resource is allocated for UE-1, the UE-1 throughput gain reaches its minimum, i.e., 35.5%.

D. Application Services over NOMA System

Based on the proposed protocol stack, various application services can be provided over our NOMA system with UE-1 and UE-2 accessing the eNB in the same experimental scenarios. The MCS of UE-1 is set to 9 and the MCS of UE-2 is set to 18. As shown in the Fig. 5, the eNB is connected to the Internet, and the UE-1 and UE-2 can access the Internet by eNB over the air at the same time. In order to further measure the over-the-air transmission rate of application layer, the SCP that is a file transmission tool in Linux is used to measure the file transfer rate from eNB to UE.

As shown in Table IV, the theoretic rate is calculated according to the TBS table [26]. The practical file transfer rate of the UE-1 is about 88.3% of the theoretic rate and the practical file transfer rate of the UE-2 is about 91.5% of the theoretic rate. As expected, the practical file transfer rate is lower than the theoretical rate. The reason can be concluded that the packet headers are not compressed yet due to the imperfect PDCP in our NOMA system. Moreover, the HARQ is not accomplished yet in our NOMA system, and the retransmission has to be carried out by the transport layer.

V. Conclusions and Outlook

In this paper, we implement a practical downlink NOMA system based on LTE specifications upon the physical layer of OAI. In our NOMA system, we focus on the SDR implementation of NOMA transceiver and the modification on protocol stack. For NOMA transceiver, a transmitter supporting signal superposition and a codeword-level SIC receiver with multi-thread processing scheme are implemented. Moreover, a new DCI format is dedicatedly designed for signal reconstitution in the developed NOMA transceiver. For another, benefit from the modified protocol stack, our NOMA system can provide various application services, such as voice, video, data and so on. Based on the developed NOMA system, a series of over-the-air experiments are carried out in our indoor experimental scenarios. The experimental results demonstrate that NOMA system achieves more than 18.6% gains in system throughput and more than 84.4% gains in cell-edge UE throughput compared with OMA system. Furthermore, two UEs can

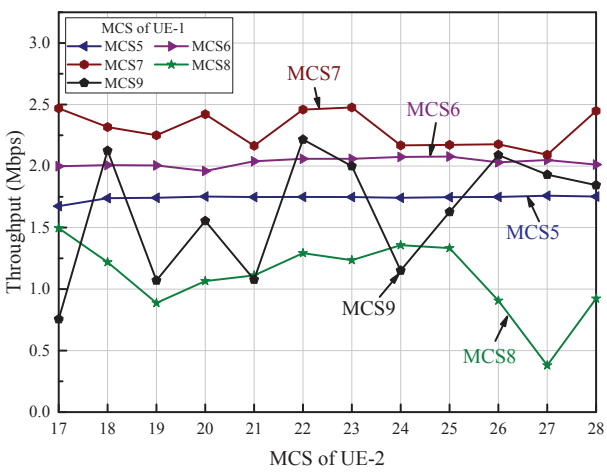

(a) UE-1 throughput.

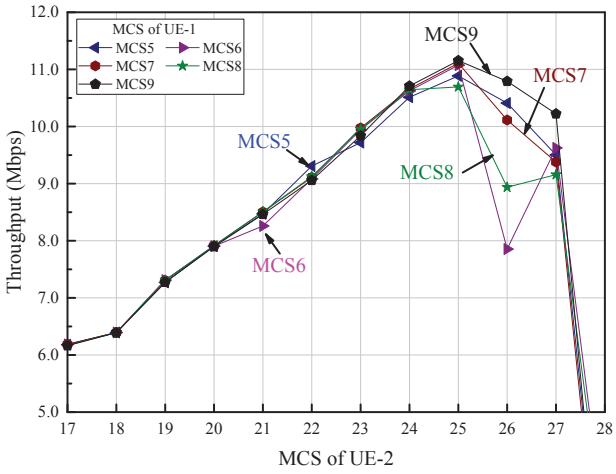

(b) UE-2 throughput.

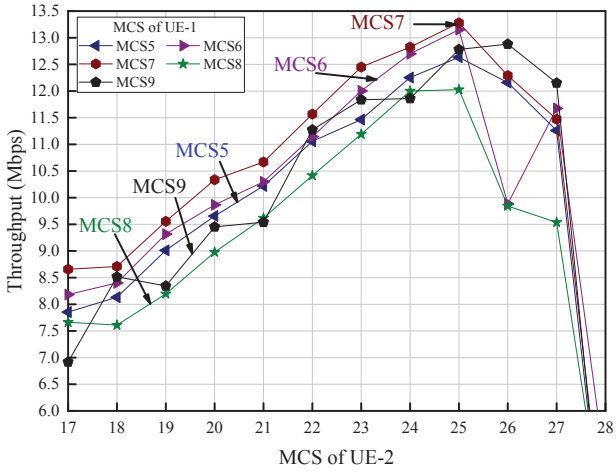

(c) System throughput.

Fig. 7. Throughput of NOMA system.

TABLE III
PERFORMANCE COMPARISONS BETWEEN OMA AND NOMA SYSTEM.

		System throughput			UE-1 throughput		
		OMA (Kbps)	NOMA (Kbps)	Gain	OMA (Kbps)	NOMA (Kbps)	Gain
Wireless resource allocation ratio for UE-1	0/8	11200.0	13279.0	18.6%	0	2172.0	–
	1/8	9850.7		34.8%	400.7		441.9%
	2/8	9201.5		44.3%	801.5		171.0%
	3/8	8202.2		61.9%	1202.2		80.7%
	4/8	7203.0		84.4%	1603.0		35.5%

TABLE IV
FILE TRANSFER RATE OF A NOMA SYSTEM.

UE	File transfer rate (Kbps)	Theoretic rate (Kbps)	Percentage
UE-1	2825.6	3206.4	88.3%
UE-2	5848.0	6393.6	91.5%

access the Internet by eNB over the air simultaneously, and the transmission rate of application layer reaches about 90% of the theoretical rate. Our developed NOMA system has further validated the feasibility of applying NOMA in practical wireless communications systems towards 5G.

For future work, the protocol stack of our NOMA system will be further optimized to improve its spectral efficiency. Furthermore, the outdoor experiments in scenarios with more users will be carried out.

VI. ACKNOWLEDGMENT

This work was supported by the National High Technology Research and Development Program of China under Grant 2014AA01A705, the China Natural Science Funding under the grant 61271183, and the Fundamental Research Funds for the Central Universities under grant 2014ZD03-02.

REFERENCES

[1] Z. Su and Q. Xu, "Content distribution over content centric mobile social networks in 5G," *IEEE Communications Magazine*, vol. 53, no. 6, pp. 66-72, Jun. 2015.

[2] Y. Saito, Y. Kishiyama, A. Benjebbour, T. Nakamura, A. Li and K. Higuchi, "Non-orthogonal multiple access (NOMA) for cellular future radio access," in *Vehicular Technology Conference (VTC Spring)*, Dresden, 2013, pp. 1-5.

[3] H. Lee, S. Kim and J. H. Lim, "Multiuser superposition transmission (MUST) for LTE-A systems," in *IEEE International Conference on Communications (ICC)*, Kuala Lumpur, 2016, pp. 1-6.

[4] K. Yakou and K. Higuchi, "Downlink NOMA with SIC using unified user grouping for non-orthogonal user multiplexing and decoding order," in *International Symposium on Intelligent Signal Processing and Communication Systems (ISPACS)*, Nusa Dua, 2015, pp. 508-513.

[5] X. Xiong, W. Xiang, K. Zheng, H. Shen and X. Wei, "An open source SDR-based NOMA system for 5G networks," *IEEE Wireless Communications*, vol. 22, no. 6, pp. 24-32, Dec. 2015.

[6] K. Zheng, S. Zhao, Z. Yang, X. Xiong and W. Xiang, "Design and implementation of LPWA-based air quality monitoring system," *IEEE Access*, vol. 4, pp. 3238-3245, Jun. 2016.

[7] N. Prasannan, G. Xavier, A. Manikkoth, R. Gandhiraj, R. Peter and K. P. Soman, "OpenBTS based microtelecom model: A socio-economic boon to rural communities," in *International Multi-Conference on Automation, Computing, Communication, Control and Compressed Sensing (iMac4s)*, Kottayam, 2013, pp. 856-861.

[8] I. Gomez-Miguelez, A. Garcia-Saavedra, P. D. Sutton, P. Serrano, C. Cano, and D. J. Leith, "srsLTE: an open-source platform for LTE evolution and experimentation," *arXiv preprint arXiv:1602.04629*, 2016.

[9] OpenAirInterface.org, Oct. 2016. [Online]. Available: http://www.openairinterface.org/

[10] N. Nikaein, M.K. Marina, S. Manickam, A. Dawson, R. Knopp, and C. Bonnet, "OpenAirInterface: a flexible platform for 5G research," *ACM SIGCOMM Computer Communication Review*, vol. 44, no. 5, pp. 33-38, Oct. 2014.

[11] A. Benjebbour, A. Li, K. Saito, Y. Saito, Y. Kishiyama and T. Nakamura, "NOMA: From concept to standardization," in *IEEE Conference on Standards for Communications and Networking (CSCN)*, Tokyo, 2015, pp. 18-23.

[12] Y. Liu, G. Pan, H. Zhang and M. Song, "On the capacity comparison between MIMO-NOMA and MIMO-OMA," *IEEE Access*, vol. 4, pp. 2123-2129, May 2016.

[13] C. Yan, A. Harada, A. Benjebbour, Y. Lan, A. Li and H. Jiang, "Receiver design for downlink non-orthogonal multiple access (NOMA)," in *IEEE 81st Vehicular Technology Conference (VTC Spring)*, Glasgow, 2015, pp. 1-6.

[14] Z. Ding, Y. Liu, J. Choi, Q. Sun, M. Elkashlan, C. I, and H. V. Poor, "Application of non-orthogonal multiple access in LTE and 5G networks," *arXiv preprint arXiv:/1511.08610*, 2015.

[15] X. Xiong, T. Wu, H. Long and K. Zheng, "Implementation and performance evaluation of LECIM for 5G M2M applications with SDR," in *IEEE Globecom Workshops (GC Wkshps)*, Austin, TX, 2014, pp. 612-617.

[16] Z. Su, Q. Xu, H. Zhu and Y. Wang, "A novel design for content delivery over software defined mobile social networks," *IEEE Network*, vol, 29, no.4, pp.62-67,Jul. 2015.

[17] S. Sesia, I. Toufik, and M. Baker, "LTE - The UMTS long term evolution: from theory to practice," 2nd ed., John Wiley & Sons, 2009, pp. 192-196.

[18] Z. Yang, Z. Ding, P. Fan, and N. Al-Dhahir, "A general power allocation scheme to guarantee quality of service in downlink and uplink NOMA systems," *IEEE Transactions on Wireless Communications*, vol. PP, no. 99, pp. 1-1, Aug. 2016.

[19] M. Zhang and S. Kim, "Universal soft demodulation schemes for M-ary phase shift keying and quadrature amplitude modulation," *IET Communications*, vol. 10, no. 3, pp. 316-326, Mar. 2016.

[20] I. Alyafawi, E. Schiller, T. Braun, D. Dimitrova, A. Gomes and N. Nikaein, "Critical issues of centralized and cloudified LTE-FDD radio access networks," in *IEEE International Conference on Communications (ICC)*, London, 2015, pp. 5523-5528.

[21] H. shen, X. Wei, H. Liu, Y. Liu, and K. Zheng, "Design and implementation of an LTE system with multi-thread parallel processing on OpenAirInterface platform," in *Vehicular Technology Conference (VTC Fall)*, Montreal, 2016.

[22] A. Masaracchia, R. Bruno, A. Passarella and S. Mangione, "Analysis of MAC-level throughput in LTE systems with link rate adaptation and HARQ protocols," in *IEEE 16th International Symposium on World of Wireless, Mobile and Multimedia Networks (WoWMoM)*, Boston, MA, 2015, pp. 1-9.

[23] R. Love, R. Kuchibhotla, A. Ghosh, R. Ratasuk, W. Xiao, B. Classon and Y. Blankenship, "Downlink control channel design for 3GPP LTE," in *IEEE Wireless Communications and Networking Conference*, Las Vegas, NV, 2008, pp. 813-818.

[24] L. Lei, Z. Zhong, K. Zheng, J. Chen and H. Meng, "Challenges on wireless heterogeneous networks for mobile cloud computing," *IEEE Wireless Communications*, vol. 20, no. 3, pp. 34-44, Jul. 2013.

[25] L. Lei, Y. Kuang, N. Cheng, X. Shen, Z. Zhong and C. Lin, "Delay-optimal dynamic mode selection and resource allocation in device-to-device communications - part 2: practical algorithm," *IEEE Transactions on Vehicular Technology*, vol. 65, no. 5, pp. 3474-3490, May 2016.

[26] Evolved Universal Terrestrial Radio Access (E-UTRA); Physical layer procedures, 3GPP TS 36.21 version 10.13.0 Release 10, 2015.